

Research Article

Physical Optics Scattering by A PEC Missile in Uniform Rectilinear Motion

Abdullah Noor, Ramazan Daşbaşı*, Burak Polat

Yildiz Technical University, Department of Electronics and Communications Engineering, Istanbul, Turkey, <https://orcid.org/0000-0002-3389-5897>, abdullah.noor@std.yildiz.edu.tr; <https://orcid.org/0000-0002-7706-2053>, rdasbasi@yildiz.edu.tr; <https://orcid.org/0000-0002-3188-2670>, abpolat@yildiz.edu.tr

* Correspondence: rdasbasi@yildiz.edu.tr

(First received March 13, 2022 and in final form June 01, 2022)

Reference: Noor, A., Daşbaşı, R., & Polat, B. Physical Optics Scattering by A PEC Missile in Uniform Rectilinear Motion. *The European Journal of Research and Development*, 2(2), 421–428.

Abstract

Electromagnetic scattering by a perfect electric conductor (PEC) missile in uniform rectilinear motion is formulated and computed in X-band under the physical optics (PO) approximation. The missile dimensions are picked as 80 [cm] in length and 6.6 [cm] in radius as adapted from the well-known Soviet M-13 missile. We adopt a canonical structure simulated by a cylindrical body, an ellipsoid nose, and four planar tail fins. The surface of the missile is meshed using triangular facets. First, the formulation and computations are carried out for a stationary missile in MATLAB™ and compared to simulations by the commercial full-wave simulator CST™. Good agreements that reveal the validity of PO formulation are observed. Finally, PO formulation and numerical results for a missile in uniform rectilinear motion are provided and discussed. These simulations are based on the principle of superposition of the formulas developed recently for scattering by a moving PEC flat plate.

Keywords: Electromagnetic Scattering, Physical Optics, Missile Radar Cross-Section, Hertzian Electrodynamics

1. Introduction

Unmanned aerial vehicles, drones, supersonic missiles, etc. come into prominence in the military industry to avoid the loss of human lives in combat. Advances in this area trigger radar manufacturers to improve their capabilities to detect such targets. Range independent radar cross-section (RCS) patterns are measures of how a target scatters the power of the incident monochromatic plane wave. RCS is a ratio of the scattered power density from the target in the direction of the receiver to the power density that is

intercepted by the target. As studied in [1] for the special case of a perfect electric conductor (PEC) plate, this quantity is time-dependent unless one may disregard the variations in the directions of the position vectors from the transmitter to the scatterer and from the scatterer to the receiver during the observation period.

We first formulate and compute electromagnetic scattering by a sample stationary PEC missile in uniform rectilinear motion in X-band under the physical optics (PO) approximation and compare the same results by the commercial full-wave electromagnetic simulator CSTTM. The surface of the missile is meshed using triangular facets. This is followed by PO formulation and discussions of numerical results for a missile in uniform rectilinear motion. These simulations are based on the principle of superposition of the formulas available in [1] and the references cited therein for scattering by a moving PEC flat plate. Time dependence is assumed $\exp(-i\omega t)$ and suppressed for the incident plane wave.

2. Physical Optics Scattering by A Stationary Missile

The canonical PEC missile under investigation, as illustrated in Fig.1, comprises a cylindrical main body, an ellipsoid nose, and four planar tail fins. Its dimensions are picked as 80 [cm] in length and 6.6 [cm] in radius as adapted from the well-known Soviet M-13 missile. Its surface is meshed into triangular facets. The missile is illuminated by a homogeneous plane wave with phasor fields (\vec{E}^i, \vec{H}^i) and propagating in \hat{n}_i – direction.

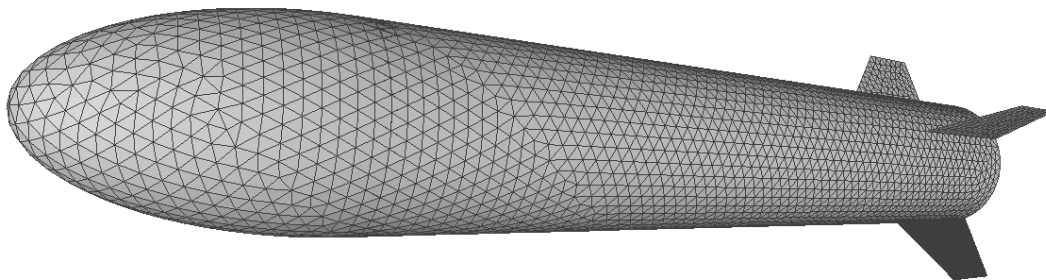


Figure 1 The 3-D model and surface meshing of the missile.

The PO surface current density function induced on an arbitrary facet is given by

$$\vec{J}_s = \begin{cases} 2\hat{n}_F \times \vec{H}^i, & \text{if facet is illuminated} \\ \vec{0}, & \text{if facet is non-illuminated} \end{cases}$$

Here, \hat{n}_F is the outward unit normal vector of a facet. An arbitrarily oriented triangular facet in a reference Cartesian frame $Ox_1x_2x_3$ is illustrated in Fig.2. The position vector of the vertices A , B , C and the center P of the triangle are represented by

$$\vec{r}_A = \hat{x}_1x_{1A} + \hat{x}_2x_{2A} + \hat{x}_3x_{3A}, \quad \vec{r}_B = \hat{x}_1x_{1B} + \hat{x}_2x_{2B} + \hat{x}_3x_{3B}, \quad \vec{r}_C = \hat{x}_1x_{1C} + \hat{x}_2x_{2C} + \hat{x}_3x_{3C}$$

and

$$\vec{r}_P = \frac{1}{3}(\vec{r}_A + \vec{r}_B + \vec{r}_C) = \hat{x}_1x_{1P} + \hat{x}_2x_{2P} + \hat{x}_3x_{3P}$$

respectively. The edge vectors between the vertices are

$$\vec{L}_{AB} = \vec{r}_B - \vec{r}_A, \quad \vec{L}_{BC} = \vec{r}_C - \vec{r}_B, \quad \vec{L}_{CA} = \vec{r}_A - \vec{r}_C.$$

Then, the unit normal vector of the facet and the area of the facet are obtained by

$$\hat{n}_F = \frac{(\vec{L}_{AB} \times \vec{L}_{BC})}{|\vec{L}_{AB} \times \vec{L}_{BC}|} = \hat{x}_1n_1 + \hat{x}_2n_2 + \hat{x}_3n_3, \quad S = \frac{1}{2}|\vec{L}_{AB} \times \vec{L}_{BC}|$$

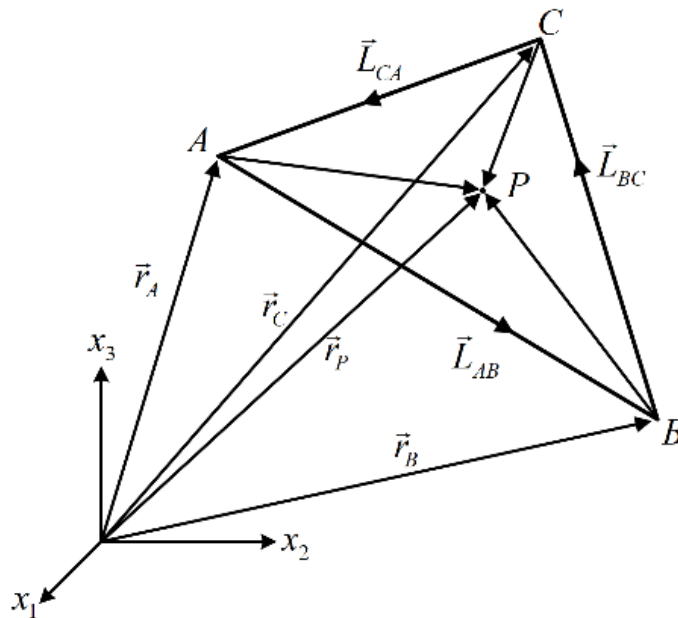


Figure 2 An arbitrarily oriented facet.

The direction of propagation of the incident wave is expressed in the reference spherical coordinates (r, θ, ϕ) by $\hat{n}_i = -\hat{r}(\theta, \phi) = -(\hat{x}_1 \sin \theta_i \cos \phi_i + \hat{x}_2 \sin \theta_i \sin \phi_i + \hat{x}_3 \cos \theta_i)$. The facet is assumed to be illuminated when $\hat{n}_i \cdot \hat{n}_F < 0$ and non-illuminated otherwise. The incident fields on a facet are expressed by

$$\vec{E}^i = (\hat{\theta}E_\theta^i + \hat{\phi}E_\phi^i)e^{i\vec{k}_i \cdot \vec{r}}, \quad \vec{H}^i = \frac{1}{Z}(\hat{n}_i \times \vec{E}^i) = \frac{1}{Z}(\hat{\theta}E_\phi^i - \hat{\phi}E_\theta^i)e^{i\vec{k}_i \cdot \vec{r}}$$

Here, $\vec{k}_i = \hat{n}_i k$ is the wave propagation vector, $k = 2\pi/\lambda$ is the wave number, and Z is the characteristic impedance of free space. The induced surface current density on the facet reads

$$\vec{J}_s = 2\hat{n}_F \times \vec{H}_i = \frac{2}{Z}\hat{n}_F \times (\hat{\theta}E_\phi^i - \hat{\phi}E_\theta^i)e^{i\vec{k}_i \cdot \vec{r}} = \frac{2}{Z}\hat{n}_F \times (\hat{\theta}E_\phi^i - \hat{\phi}E_\theta^i)e^{-ikh}$$

with

$$h = -\hat{n}_i \cdot \vec{r}_p = (\hat{x}_1 \sin \theta_i \cos \phi_i + \hat{x}_2 \sin \theta_i \sin \phi_i + \hat{x}_3 \cos \theta_i) \cdot (\hat{x}_1 x_{1p} + \hat{x}_2 x_{2p} + \hat{x}_3 x_{3p})$$

The PO scattered electric field is given by the integral

$$\vec{E}^s = \frac{-ikZ}{4\pi r} e^{ikr} \iint_{S_F} \vec{J}_s e^{-ikg} dS$$

over the surface of the facet S_F under the far field approximation with

$$g = \hat{r} \cdot \vec{r}_p = (\hat{x}_1 \sin \theta \cos \phi + \hat{x}_2 \sin \theta \sin \phi + \hat{x}_3 \cos \theta) \cdot (\hat{x}_1 x_{1p} + \hat{x}_2 x_{2p} + \hat{x}_3 x_{3p})$$

This integral is computed numerically by the method given [2] after transforming the facet to simplex coordinates as in [3], [4].

3. The Influence of Uniform Rectilinear Motion

We consider the special case when the missile is in rectilinear motion in a particular direction \hat{v} with a velocity vector $\vec{v} = \hat{v}G$, $G = \text{fixed}$. The PO approximation enables us to express the Doppler mechanism on each facet by that on an infinite PEC plane, as illustrated in Fig.3 for the special case of TM incidence.

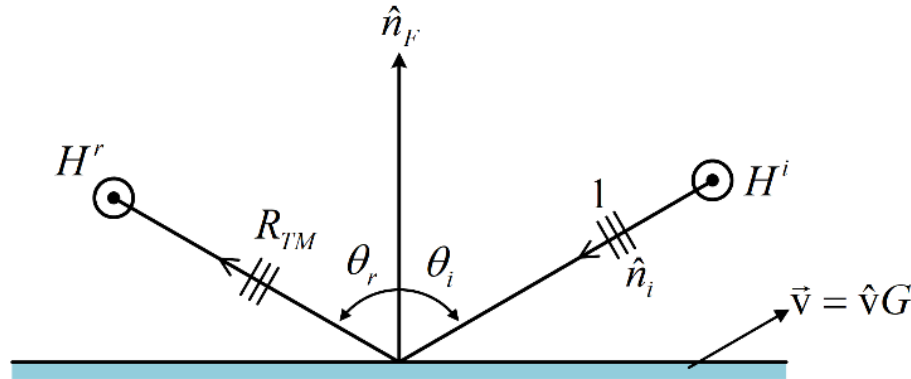


Figure 3 TM Plane wave incidence on a PEC plane in uniform rectilinear motion.

We decompose the arbitrary direction of wave incidence $\hat{n}_i = \hat{t}_{Fn}n_t + \hat{n}_Fn_n$ and velocity vector of the facet $\vec{v} = \hat{v}G = (\hat{t}_{Fv}v_t + \hat{n}_Fv_n)G$ into their tangential (t) and normal (n) components w.r.t. the PEC plane. As investigated in [5], the Doppler mechanisms for the angle of reflection, reflection coefficients for TE and TM polarizations, and the angular frequency of the reflection wave read

$$\sin \theta_r = \frac{\sin \theta_i}{1 + 2\beta \sin \theta_i}, \quad R_{TM} = \frac{\cos \theta_i}{\cos \theta_r}, \quad R_{TE} = -1, \quad \omega_r = \frac{\omega_i}{1 + 2\beta \sin \theta_i}$$

Here, $\beta = -(\hat{t}_{Fn} \cdot \hat{t}_{Fv}v_t)G/c$ while $c \approx 3 \times 10^8$ [m/s] is the phase velocity of propagation in free space. When $\hat{t}_{Fn} \cdot \hat{t}_{Fv}v_t$ is not fixed for every facet on the target - as is the case for volumetric bodies or non-planar surfaces - the total scattered wave is non-monochromatic as each facet may generate separate Doppler mechanisms.

4. Results

Our first numerical investigation is a MATLABTM code that computes PO scattering from the stationary missile. The missile in Fig.1 is oriented along x_2 - axis and meshed by 23644 triangular facets having common edge length of ≈ 6.5 [mm]. A $f = 10$ [GHz] plane wave is incident with $\theta_i = 45^\circ$, $\phi_i = 0^\circ$. The PO code is executed in the range of observation $\theta_i \in (-180^\circ, 180^\circ]$ with $\Delta\theta = 1^\circ$ angular step width, while $\phi = 0^\circ$ (fixed). This scenario is also simulated by the commercial electromagnetic simulation software CSTTM Studio Suite. The normalized patterns of both simulations are depicted in Fig.4a, where we observe a good match.

Next, $\vec{v} = -\hat{x}_1 c/10$ velocity vector is picked for the missile and simulated in the time interval $t = 0, 200$ [ps] with $\Delta t = 12.5$ [ps] steps using PO. The motion of the missile shifts the reflection angle from -135° to -129° at $t = 0$ [s] and amplifies the reflection coefficient about 1 [dB] as depicted in Fig.4b. The total scattered wave is no longer monochromatic. The normalized frequency spectrum of the total scattered electric field is obtained by Fast Fourier Transform operation in MATLABTM with $f_s = 8f$ sampling frequency and depicted in Fig.5. The maximum amplitude is observed at 11 [GHz] and -131° .

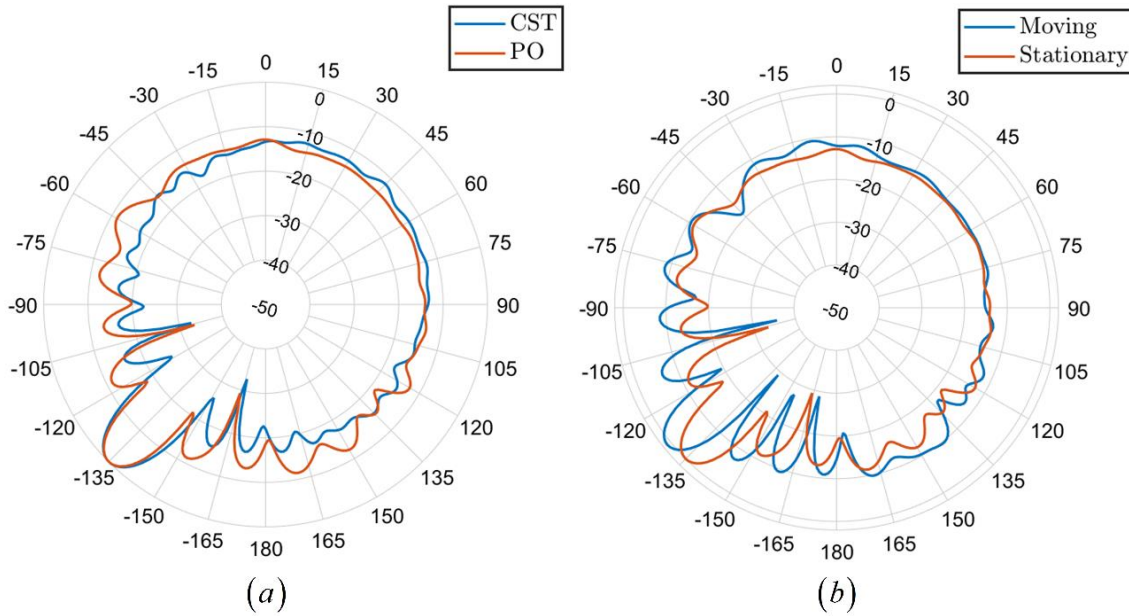


Figure 4 Normalized scattering patterns (a) for a stationary missile by CSTTM vs. PO (b) for a moving missile with $\vec{v} = -\hat{x}_1 c/10$ vs. stationary missile by PO.

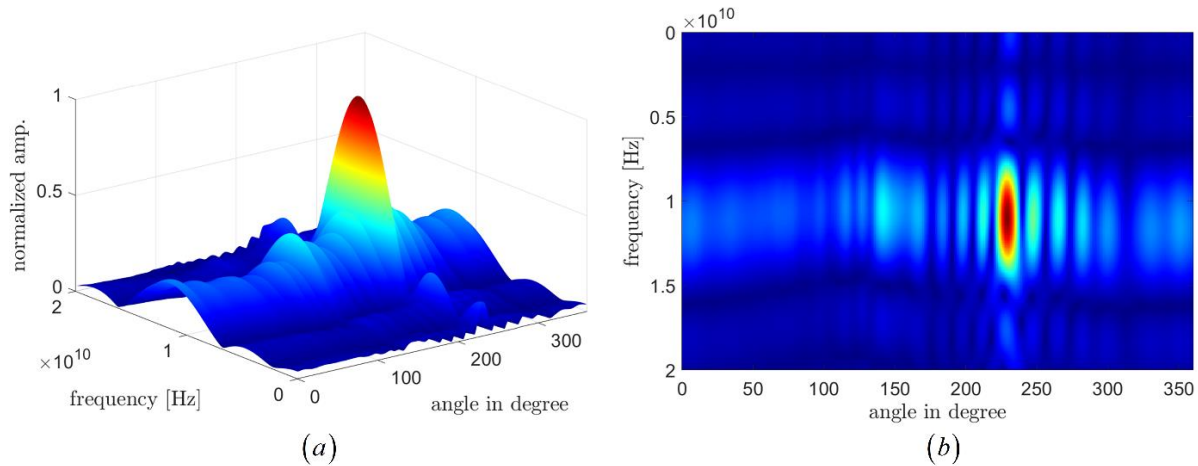


Figure 5 Normalized spectrum of the total scattered electric field by a moving missile with $\vec{v} = -\hat{x}_1 c/10$ (a) 3-D view (b) 2-D view

If the direction of velocity vector is reversed as $\vec{v} = \hat{x}_1 c/10$ in the simulation, while all other parameters kept unchanged, the motion of the missile shifts the reflection angle in opposite direction (to that in the previous case) from -135° to -139° at $t=0[s]$ and attenuates the reflection coefficient about 1.8 [dB], as observed in Fig.6b. The normalized frequency spectrum of the total scattered field is depicted in Fig.7. The maximum amplitude is observed at 9.6 [GHz] and -137° .

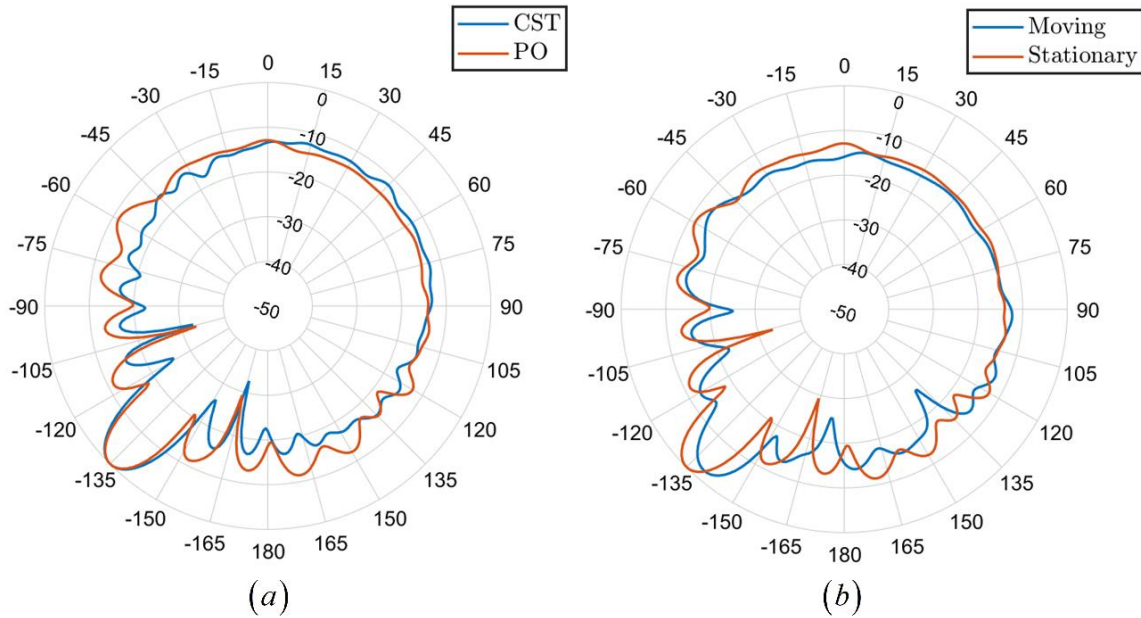


Figure 6 Normalized scattering patterns (a) for a stationary missile by CSTTM vs. PO (b) for a moving missile with $\vec{v} = \hat{x}_1 c/10$ vs. stationary missile by PO.

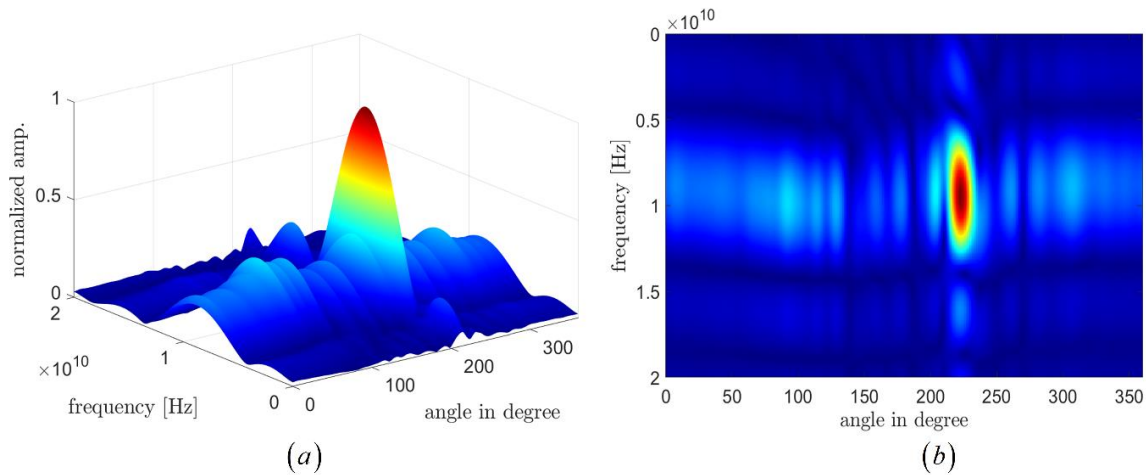


Figure 7 Normalized spectrum of the total scattered electric field by a moving missile with $\vec{v} = \hat{x}_1 c/10$ (a) 3-D view (b) 2-D view

5. Conclusion

In this paper, PO scattering from a missile in uniform rectilinear motion is developed and computed in X-band. Comparative results with full wave simulator CSTTM are also provided for the stationary case. The Doppler shifts in the scattering patterns agree with similar observations for an infinite PEC plane. The investigation is planned to be extended to non-PEC platforms such as impedance and transmissive surfaces, also considering asymptotic contributions by edge and multiple diffraction mechanisms.

Acknowledgement

This work was supported by Research Fund of the Yildiz Technical University. Project Number: FBA-2021-4310.

References

- [1] Polat, B. and Daşbaşı R., (2021), "Free Space Doppler Analysis and RCS of a Moving PEC Plate Under Physical Optics Approximation" Proceedings of 8th International Conference on Electrical and Electronics Engineering (ICEEE) Antalya, Turkey April 9-11, pp.27-31.
- [2] Moreira F. J. S., and Prata A., (1994), A Self-checking Predictor-Corrector Algorithm for Efficient Evaluation of Reflector Antenna Radiation Integrals, IEEE Transactions on Antennas and Propagation Vol. 42, no. 2.
- [3] Gibson W. C., (2008), The Method of Moments in Electromagnetics, Chapman & Hall/CRC.
- [4] Garrido E. E., (2000), Graphical user interface for a physical optics radar cross section prediction code," Master Thesis, Naval Postgraduate School.
- [5] Polat, B., (2012), Scattering by a Moving PEC Plane and a Dielectric Half-Space in Hertzian Electrodynamics, TWMS Journal of Applied and Engineering Mathematics, vol.2, no.2, pp.123-144